# Human DNA Polymerases λ and β Show Different Efficiencies of Translesion DNA Synthesis past Abasic Sites and Alternative Mechanisms for Frameshift Generation†

Giuseppina Blanca,‡ Giuseppe Villani,‡ Igor Shevelev,§ Kristijan Ramadan,§ Silvio Spadari,|| Ulrich Hübscher,§ and Giovanni Maga*,||

*Institut de Pharmacologie et de Biologie Structurale, Centre National de la Recherche Scientifique, 205 route de Narbonne, 31077 Toulouse Cedex, France, Institute of Veterinary Biochemistry and Molecular Biology IVB-MB, University of Zürich, Winterthurerstrasse 190, CH-8057 Zürich, Switzerland, and Istituto di Genetica Molecolare IGM-CNR, National Research Council, via Abbiategrasso 207, 27100 Pavia, Italy*

*Received May 11, 2004; Revised Manuscript Received July 6, 2004*

ABSTRACT: Human DNA polymerases (pols) β and λ could promote template slippage and generate −1 frameshifts on defined heteropolymeric DNA substrates containing a single abasic site. Kinetic data demonstrated that pol λ was more efficient than pol β in catalyzing translesion DNA synthesis past an abasic site, particularly in the presence of low nucleotide concentrations. Moreover, pol λ was found to generate frameshifts in two ways: first, by using a nucleotide-stabilized primer misalignment mechanism, or second, by promoting primer reannealing using microhomology regions between the terminal primer sequence and the template strand. Our results suggest a molecular mechanism for the observed high in vivo rate of frameshifts generation by pol λ and highlight the remarkable ability of pol λ to promote microhomology pairing between two DNA strands, further supporting its proposed role in the nonhomologous end joining process.

Family X DNA polymerases (pols)[1] are present in different organisms ranging from viruses to higher eukaryotes (*1*), but the members of this family vary considerably in their properties. The best characterized is pol β, which is essential for base excision repair (BER) and nucleotide excision repair (NER) pathways and whose structure has been resolved in the absence of substrates (*2*, *3*) and as different binary and ternary complexes (*4*, *5*).

Pol λ is another family X member that is present in higher eukaryotes. It is similar in sequence to pol β and terminal deoxynucleotidyl transferase (TdT) and shares many structural and biochemical properties with pol β (*6*, *7*) and with TdT (*8*). Pol λ has a high affinity for dNTPs, leading to the suggestion that it can work efficiently when intracellular dNTP concentrations are low (*9*). The observation that pol λ has an extraordinary ability to generate frameshift errors (*10*) may be a consequence of its DNA binding mode. The recently solved structure of pol λ (*11*) showed that this enzyme can adopt a closed active conformation in the absence of an incoming dNTP and that it loosely interacts with the template backbone, suggesting that the mode of binding of pol λ with the DNA is intermediate between those of pol β, which has more extensive interactions with the template, and TdT, which has none. Indeed, it has been suggested that TdT remains in a closed active conformation throughout its catalytic cycle (*12*), and this might be essential to overcome the difficulties inherent to an untemplated reaction. Interestingly, also the Y family polymerases have been suggested to exist in a closed conformation in the absence of bound substrates (for review see ref *13*). These enzymes have been shown to possess low fidelity of DNA synthesis (*14*), a property which has been related to their ability to carry on DNA synthesis in the presence of a variety of DNA lesions, and therefore are called translesion (TLS) pols. However, also pol β and pol λ, whose fidelity of DNA synthesis is higher than those of the family Y pols, can bypass certain DNA lesions, in particular AP sites (*15*, *16*).

Loss of purine and pyrimidine bases is a significant source of DNA damage in prokaryotic and eukaryotic organisms. Abasic (apurinic and apyrimidinic) lesions occur spontaneously in DNA; in eukaryotes it has been estimated that about $10^4$ depurination and $10^2$ depyrimidation events occur per day (*17*). An equally important source of abasic DNA lesions results from the action of DNA glycosylases, such as uracil glycosylase, which excises uracil arising primarily from spontaneous deamination of cytosine (*18*). DNA with AP lesions presents a strong block to DNA synthesis by replicative pols. Although most AP sites are removed by the BER pathway, a small fraction of lesions persists (*19*). These AP sites are replicated by TLS pols with a high probability

† This work was supported by the EU (Project QLK3-CT-202-02071 REBIOTECH) to G.M. and U.H., the CARIPLO Foundation Project Oncogenetica e Proteomica della Replicazione (2003.1663/10.8441) to G.M., Grant 3447 from the Association pour la recherche sur le Cancer to G.V., the Swiss National Science Foundation (Grant 3100.061361.00) to K.R. and U.H., the BBW (02.2286) to U.H. and K.R., and the Kanton of Zürich to G.M. and U.H. G.B. is supported by a posdoctoral fellowship from the French Ministére de la Recherche Scientifique.

* Corresponding author: e-mail, maga@igm.cnr.it; fax, 39-03824-22286; phone, 39-0382546354.

‡ Centre National de la Recherche Scientifique.

§ University of Zürich.

|| National Research Council.

[1] Abbreviations: pol, DNA polymerase; TdT, 3′-terminal deoxynucleotidyl transferase; dNTP, deoxynucleoside triphosphate; AP, abasic site; TLS, translesion; ss, single stranded; ds, double stranded; nt, nucleotide.

10.1021/bi049050x CCC: $27.50 
Published on Web 08/20/2004

to establish a mutation. Studies with purified prokaryotic and viral pols showed that incorporation of A opposite AP sites occurs about 10-fold more frequently than G opposite the lesion and about 50-fold more frequently than either C or T (*20*). NMR studies showed that when A is opposite an abasic lesion, it stacks in an intrahelical configuration causing virtually no distortion of the DNA helix, providing a physical basis for this preferential incorporation of A opposite AP lesions, which is referred to as the "A-rule". Until recently, it was assumed that pols and reverse transcriptases generally behave in accordance with the A-rule when challenged with an AP site.

However, the recently solved structures of an archeal family Y pol, Dpo4 from *Sulfolobus solfataricus*, and of the family B pol from the bacteriophage RB69, in complex with different AP site-containing DNA substrates, provided evidence for different molecular mechanisms of AP site bypass (*21*, *22*). The main observation was that translesion synthesis was preferentially template directed with the AP site looped out and the incoming nucleotide opposite the base 5′ to the lesion. The resulting DNA synthesis generated a −1 frameshift when the AP site was extrahelical. Template realignment during primer extension was also observed, resulting in base substitutions or even +1 frameshifts. Interestingly, enzymological studies showed that AP site bypass by pol $\beta$ occurred predominantly by "skipping over" the lesion, inserting a nucleotide complementary to an adjacent downstream template base. This "dNTP-stabilized" mechanism, analogous to but different from the classical template slippage, resulted in both deletion and base substitution errors (*15*). On the other hand, no detailed mechanistic studies have been reported for AP site bypass by pol $\lambda$. In light of these considerations, we investigated the molecular mechanism underlying the ability of pol $\beta$ and pol $\lambda$ to bypass an AP site and to generate frameshift errors. Our data suggest that pol $\beta$ and pol $\lambda$ have alternative mechanisms for frameshift generations.

## MATERIALS AND METHODS

*Chemicals.* [$\gamma$-$^{32}$P]ATP (3000 Ci/mmol) was from Amersham; unlabeled dNTPs were from Roche Molecular Biochemicals. The tetrahydrofuran (dSpacer) was from Glen Research. Whatman was the supplier of the GF/C filters. All other reagents were of analytical grade and were purchased from Merck or Fluka.

*Nucleic Acid Substrates.* The 73mer and 60mer DNA oligonucleotides, either undamaged or containing the synthetic (tetrahydrofuran) AP site, and the corresponding primers were chemically synthesized and purified on denaturing polyacrylamide gel. The sequence for the d73mer is 5′GATCGGGAGGGTAGGAATATTGAG[**X**/**G**]ATGAAGGGTTGAGTTGAGTGGAGATAGTGGA*GGGTAGTATGGTGGATA*3′. The sequences complementary to the 17-mer and 18-mer primers are underlined and italicized, respectively. In brackets, the position of the lesion or the corresponding G residue in the undamaged template is indicated in bold letters (X, AP site). The sequence of the 60-mer ss oligonucleotide was 5′CAATGATCTCGTCAGCATCT[**X**/**G**]TGTGAATTCGGCACTGGCCGTC*GTATGCTCTTGGTTGTA*3′. The sequences complementary to the 17-merand 20-mer primers are underlined and italicized, respectively. In brackets, the position of the lesion or the corresponding G residue in the undamaged template is indicated in bold letters (X, AP site).

*Enzymes and Proteins.* Recombinant human wild-type pol $\lambda$ was expressed and purified as described (*16*). After purification, the protein was >90% homogeneous, as judged by SDS−PAGE and Coomassie staining, and had a specific activity of 200000 units/mg. Recombinant pol $\beta$ was purchased from Trevigen and had a specific activity of 60000 units/mg. One unit of pol activity corresponds to the incorporation of 1 pmol of total dTMP into acid-precipitable material in 60 min at 37 °C in a standard assay containing 0.5 $\mu$g (as nucleotides) of poly(dA)/oligo(dT)$_{10:1}$ and 10 $\mu$M dTTP.

*Enzymatic Assays: DNA Polymerase Assay.* Pol $\lambda$ activity was assayed in a final volume of 10 $\mu$L containing 50 mM Tris-HCl (pH 7.0), 0.25 mg/mL BSA, 1 mM DTT, and 0.5 mM $MnCl_2$. Enzymes, unlabeled dNTPs, and template concentrations were as indicated in the figure legends. All reactions were incubated for 15 min at 37 °C unless otherwise stated and resolved on 14% polyacrylamide−7 M urea−30% formamide gels in 89 mM Tris-HCl, pH 9.0, 28 mM taurine, and 0.2 mM EDTA (United States Biochemicals). Reactions products were visualized and quantified by storage phosphor analysis with a Molecular Dynamics Storm 820 using ImageQuant version 5.2 software.

*Kinetic Analysis.* For quantification of the reaction products after separation on the sequencing gels, the products were calculated from the values of integrated gel band intensities $I^*_T/I_{T-1}$, where $T$ = target site, the template position of interest, and $I^*_T$ = the sum of the integrated intensities at positions $T$, $T + 1$, ..., $T + n$. All of the intensity values were normalized to the total intensity of the corresponding lane to correct for differences in gel loading. An empty lane was scanned and the corresponding value subtracted as background.

Initial velocities of the reactions were derived from single time point experiments, which corresponded to the mid-time points of the linear range of the reactions, as previously determined (data not shown). The $K_m$ and $V_{max}$ values were calculated by plotting the initial velocities in dependence of the substrate concentrations and fitting the data according to the Michaelis−Menten equation in the form:

$$v = \frac{k_{cat}E_0}{1 + K_m/[S]}$$

where $k_{cat}E_0 = V_{max}$. For substrate inhibition studies, the experimental data were analyzed with the equation:

$$v = \frac{k_{cat}E_0}{1 + K_m/[S] + [S]/K_i}$$

Nonlinear least-squares curve fitting was done with the software GraphPad Prism.

## RESULTS

*Pol $\lambda$ and Pol $\beta$ Generate −1 Frameshifts during Abasic Site Bypass.* Both pol $\beta$ and pol $\lambda$ are able to bypass abasic (AP) sites in vitro. First, we have compared the AP site

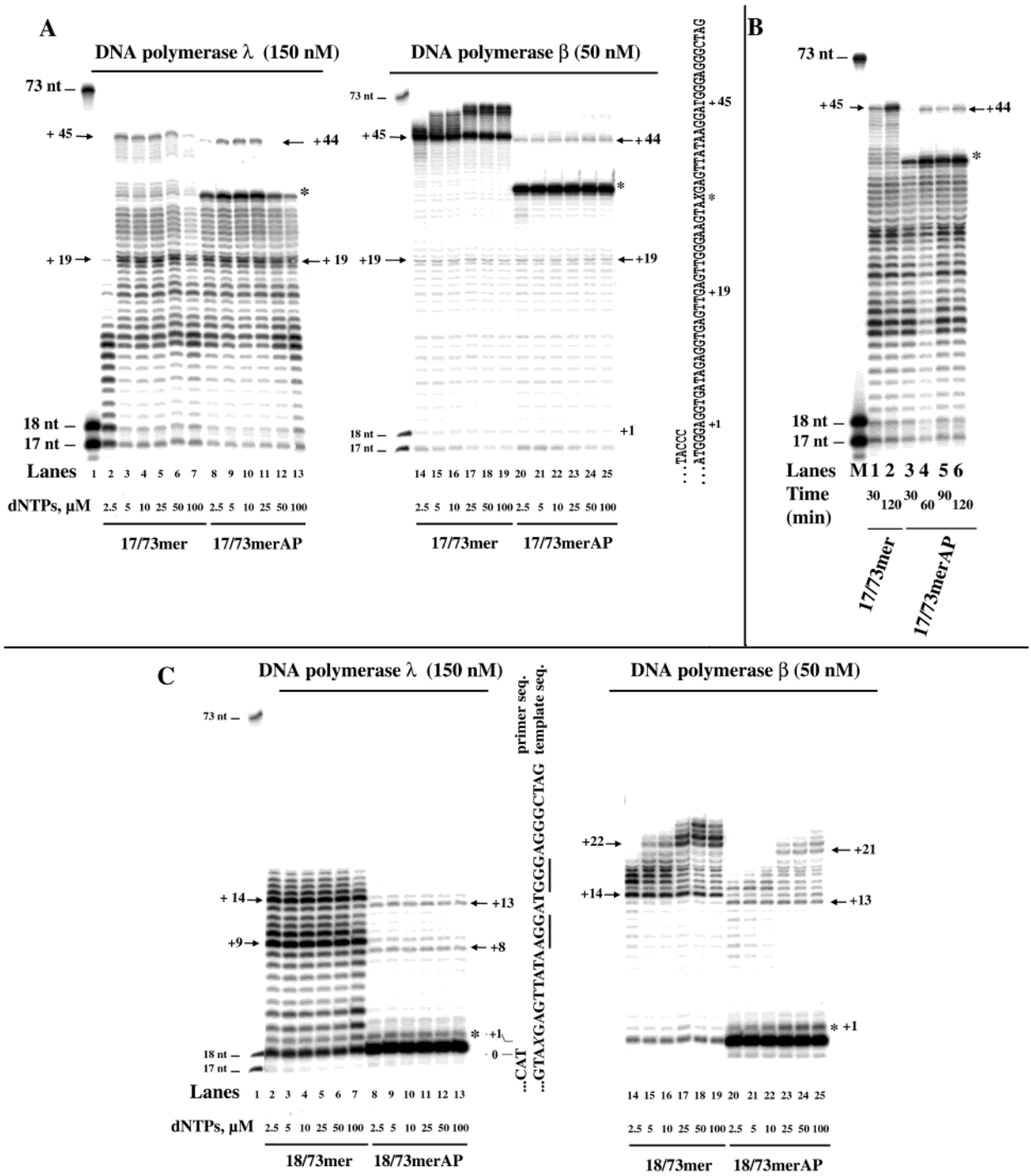


FIGURE 1: DNA polymerases $\beta$ and $\lambda$ generate a $-1$ frameshift in the presence of an AP site. (A) DNA primer elongation by pol $\lambda$ (lanes 2−13) and pol $\beta$ (lanes 14−25) was measured under running start conditions, as described in Materials and Methods, in the presence of increasing amounts of dNTPs and 0.2 pmol of the 17/73mer heteropolymeric DNA primer/template, either undamaged (lanes 2−7, 14−19) or containing a single AP site (lanes 8−13, 20−25). The enzyme concentrations used are indicated on the top of the figure. Oligonucleotide size markers are in lane 1. Arrows indicate the position of pausing sites. The asterisk indicates the position of the AP site. The sequence of the DNA template is indicated on the right side of the panel. X = G in the undamaged template or AP site in the damaged template. (B) Time-dependent DNA primer elongation by pol $\lambda$ (150 nM) was measured under running start conditions, as described in Materials and Methods, in the presence of 5 $\mu$M dNTPs and 0.2 pmol of the 17/73mer heteropolymeric DNA primer/template, either undamaged (lanes 1 and 2) or containing a single AP site (lanes 3−6). Incubation times are indicated at the bottom of the figure. Lane M shows oligonucleotide size markers. Arrows indicate the position of pausing sites. The asterisk indicates the position of the AP site. (C) DNA primer elongation by pol $\lambda$ (lanes 2−13) and pol $\beta$ (lanes 14−25) was measured under standing start conditions, as described in Materials and Methods, in the presence of increasing amounts of dNTPs and 0.2 pmol of the 18/73mer heteropolymeric DNA primer/template, either undamaged (lanes 2−7, 14−19) or containing a single AP site (lanes 8−13, 20−25). The pol concentrations used are indicated at the top of the figure. Lane 1 shows oligonucleotide size markers. Arrows indicate the position of pausing sites. The sequence of the DNA template is indicated in the middle of the panel, with the major pausing sites underlined. X = G in the undamaged template or AP site in the damaged template.

bypass capacity of both enzymes as a function of the nucleotide concentration, on a 17/73mer heteropolymeric DNA substrate, either undamaged or containing a single AP site (see Materials and Methods for the complete sequence

of the primer/template). As shown in Figure 1A, synthesis by pol $\lambda$ on the undamaged template (lanes 2−7) was distributive, with several pausing sites. In particular, a strong stop was observed after the incorporation of 19 nt (indicated on the left side of Figure 1A as +19) and synthesis was completely terminated at position +45, immediately preceding the first of two neighboring GGG triplets in the template sequence. When this experiment was repeated with the same DNA template, but bearing a single AP site at position +32 from the 3′-OH of the primer, that is under running start conditions (lanes 8−13), a strong stop was observed at the position immediately preceding the lesion. However, the synthesis eventually continued past the AP site but terminated with a +44 product instead of the expected +45 observed in the absence of the AP site. Interestingly, the products synthesized before the lesion were undistinguishable from the corresponding products synthesized on the undamaged template. This is exemplified by the presence of the same pausing site at position +19 (compare lanes 2−7 with lanes 8−13). Since the sequence was the same for both templates, these results suggested that the presence of the AP site induced a −1 frameshift during replication by pol $\lambda$. Next, similar experiments were performed with pol $\beta$. As a general consideration, pol $\beta$ was less sensitive to the pausing site at position +45, being able to synthesize longer products than pol $\lambda$ (Figure 1A, lanes 14−19). As shown in Figure 1A, under running start conditions (lanes 14−25) pol $\beta$ showed a −1 frameshift in the presence of an AP site, as can be seen by the shortening of the main product accumulated during the pausing of the enzyme, from +45 with the undamaged 17/73mer substrate (lanes 14−19) to +44 with the damaged substrate (lanes 20−25). Figure 1B shows that, even after 2 h of incubation, the products synthesized by pol $\lambda$ on the 17/73mer DNA substrate with the single AP site (lanes 3−6) were 1 nt shorter than the corresponding products on the undamaged one (lanes 1 and 2).

Next, to confirm the capacity of the AP site to generate a −1 frameshift, AP bypass by both pol $\beta$ and pol $\lambda$ was studied under standing start conditions. For this, an 18mer primer was annealed to the same 73mer template to generate an 18/73mer DNA substrate where the AP site was at position +1 from the 3′-OH of the primer (see Materials and Methods for the complete sequence of the primer/template). When pol $\lambda$ was tested on the undamaged 18/73mer template (Figure 1C, lanes 2−7) a strong accumulation of a +9 product (corresponding to pausing in front of an AGG triplet) and a +14 product (corresponding to pausing in front of a GGG triplet) was observed. When the same experiment was performed in the presence of the 18/73mer substrate with the AP site at position +1 (lanes 8−13), the overall efficiency of DNA synthesis was reduced to less than 10%, and the bypass products were 1 nt shorter than the corresponding ones on the undamaged template. This was evident by the −1 shift of the two strong pausing sites, which now appeared as +8 and +13 products. Eventually, synthesis stopped in front of the GGG triplet. This further reinforced the notion that the presence of an AP site induced a −1 frameshift by pol $\lambda$. Pol $\beta$ also generated a −1 frameshift when copying an AP site under standing start conditions (Figure 1C). This was monitored by the shortening of the products that accumulated during the pausing of the enzyme, which went from +14 and +22 with the undamaged 18/73mer substrate (lanes 14−19) to +13 and +21 with the damaged substrate (lanes 20−25). In summary, these results suggested that both pol $\lambda$ and pol $\beta$ can bypass the AP site, thus generating a −1 frameshift.

Table 1: Kinetic Parameters for dNTP Incorporation by DNA Polymerases $\beta$ and $\lambda$ during Normal and Translesion DNA Synthesis

| | Pol $\lambda$ | | | |
|---|---|---|---|---|
| | 17/73 | | 18/73 | |
| | undamaged[a] | AP damaged[a] | undamaged | AP damaged |
| $K_m$ ($\mu$M) | 0.2 | 0.04 | 0.3 | 0.06 |
| $k_{cat}$ (min$^{-1}$) | 0.014 | 0.004 | 0.055 | 0.017 |
| $k_{cat}/K_m$ | 0.07 | 0.1 | 0.18 | 0.28 |
| $K_i$ ($\mu$M) | 860 | 62 | 590 | 56 |

| | Pol $\beta$ | | | |
|---|---|---|---|---|
| | 17/73 | | 18/73 | |
| | undamaged[a] | AP damaged[a] | undamaged | AP damaged |
| $K_m$ ($\mu$M) | 0.44 | 1.5 | 0.4 | 2.2 |
| $k_{cat}$ (min$^{-1}$) | 0.51 | 0.02 | 0.19 | 0.03 |
| $k_{cat}/K_m$ | 1.16 | 0.013 | 0.47 | 0.014 |

Relative Efficiency (Damaged vs Undamaged)

| | 17/73 $(k_{cat}/K_m)_{AP}/(k_{cat}/K_m)_C$[b] | 18/73 $(k_{cat}/K_m)_{AP}/(k_{cat}/K_m)_C$ |
|---|---|---|
| pol $\lambda$ | 1.4 | 1.5 |
| pol $\beta$ | 0.01 | 0.03 |

Absolute Efficiency (Pol $\lambda$ vs Pol $\beta$)

| | 17/73 $(k_{cat}/K_m)\lambda/(k_{cat}/K_m)\beta$ | 18/73 $(k_{cat}/K_m)\lambda/(k_{cat}/K_m)\beta$ |
|---|---|---|
| C | 0.06 | 0.4 |
| AP | 7.7 | 20 |

[a] Relative to the translesion synthesis from position 49 to the end. [b] AP = AP-damaged DNA; C = undamaged control DNA.

*Pol $\lambda$ Shows Higher Affinity for the Nucleotide Substrate and Higher Efficiency of AP Site Bypass Than Pol $\beta$.* Quantification of the products synthesized in the absence or in the presence of an AP site as a function of the nucleotide (dNTP) concentrations allowed us to derive the steady-state kinetic parameters for normal and translesion DNA synthesis by pol $\beta$ and pol $\lambda$. The calculated kinetic constants ($K_m$, $k_{cat}$, $k_{cat}/K_m$) are summarized in Table 1. Pol $\beta$ showed an higher apparent rate of nucleotide incorporation ($k_{cat}$) than pol $\lambda$. In addition, the $k_{cat}$ was decreased for both pols by the presence of an AP site, consistent with the notion that a lesion in the template strand is detrimental to the enzyme's catalytic efficiency. However, the decrease in $k_{cat}$ was higher for pol $\beta$, under both standing start and running start conditions (between 6- and 25-fold), than for pol $\lambda$ (3-fold). When looking at the apparent affinities for the nucleotide substrate ($K_m$), another important difference could be observed, namely, that the presence of an AP site apparently decreased the affinity of pol $\beta$ for the dNTPs (as shown by the 4−5-fold increase in the $K_m$ values), whereas, on the other hand, the affinity was increased for pol $\lambda$ (which showed a 5-fold decrease in the $K_m$ values). When the relative efficiency of nucleotide incorporation ($k_{cat}/K_m$ values) was compared for the undamaged vs the damaged DNA template (Table 1), it can be seen that pol $\lambda$ was equally effective in replicating both templates, whereas pol $\beta$ preferred 25−30-fold the undamaged template. As a consequence, pol $\lambda$ was 7.7−20-fold more efficient in replicating an AP site contain-

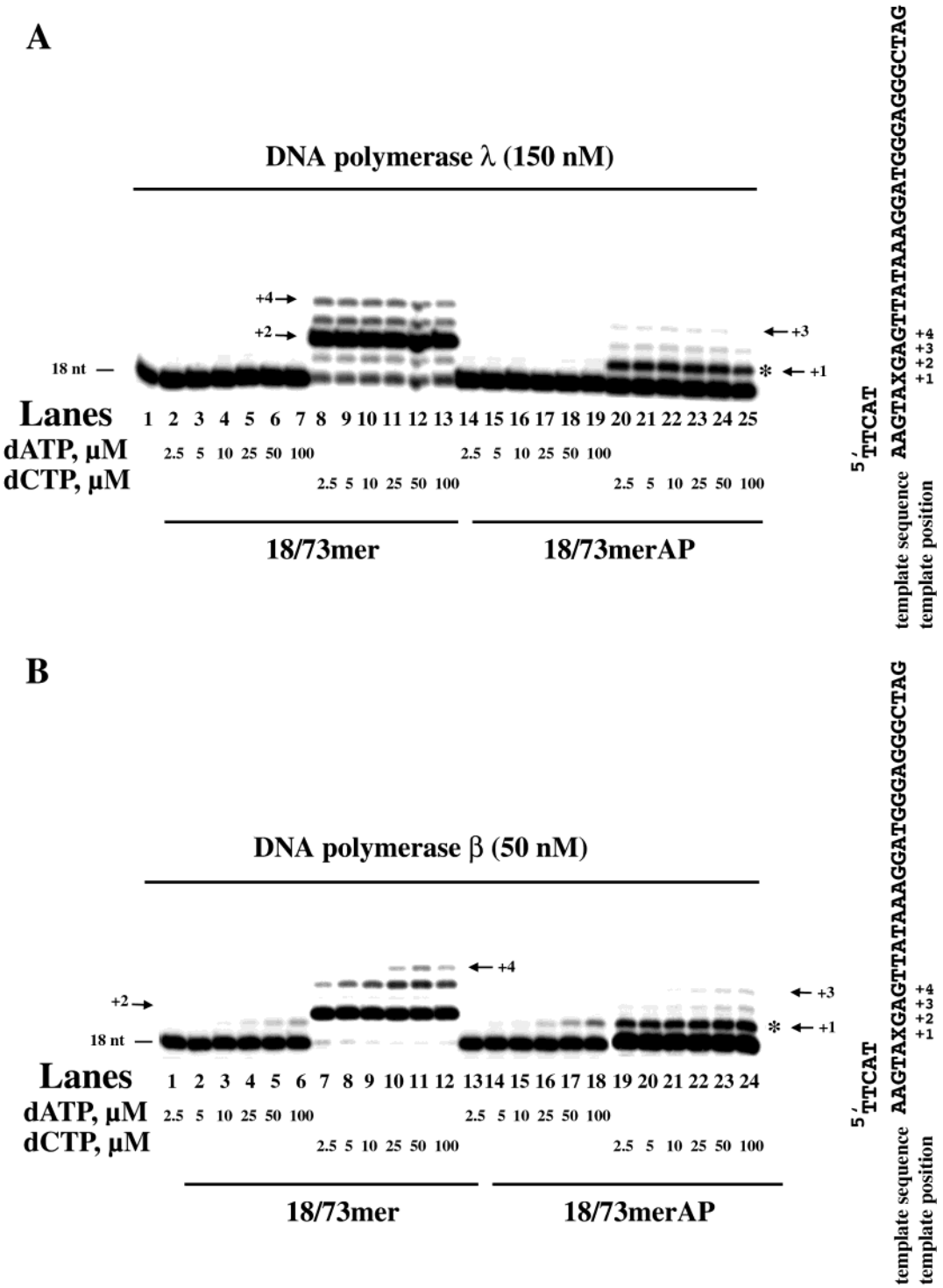


FIGURE 2: DNA polymerase $\beta$, but not DNA polymerase $\lambda$, can bypass an AP site by two alternative mechanisms. (A) DNA primer elongation by pol $\lambda$ was measured under standing start conditions, as described in Materials and Methods, in the presence of 0.2 pmol of the 18/73mer heteropolymeric DNA primer/template, either undamaged (lanes 2−13) or containing a single AP site (lanes 14−25), and in the presence of increasing amounts of either dATP (lanes 2−7, 14−19) or dCTP (lanes 8−13, 20−25). The amount of pol $\lambda$ used is indicated at the top of the figure. Lane 1 shows the 18mer oligonucleotide size marker. Arrows indicate the position of pausing sites. The asterisk indicates the position of the AP site. The sequence of the DNA template is indicated on the left side of the panel. X = G in the undamaged template or AP site in the damaged template. (B) DNA primer elongation by pol $\beta$ was measured under standing start conditions, as described in Materials and Methods, in the presence of 0.2 pmol of the 18/73mer heteropolymeric DNA primer/template, either undamaged (lanes 1−12) or containing a single AP site (lanes 13−24), and in the presence of increasing amounts of either dATP (lanes 1−6, 13−18) or dCTP (lanes 7−12, 19−24). The amount of pol $\beta$ used is indicated at the top of the figure. Arrows indicate the position of pausing sites. The asterisk indicates the position of the AP site. The sequence of the DNA template is indicated on the left side of the panel. X = G in the undamaged template or AP site in the damaged template.

ing DNA template than pol $\beta$. As shown in Figure 1A, pol $\lambda$ was inhibited by high concentrations of dNTPs. By using the appropriate kinetic model (see Materials and Methods), it was possible to estimate the apparent inhibition constant ($K_i$) for this substrate inhibition effect. Pol $\lambda$ activity was inhibited by dNTP concentration above 50−60 $\mu$M (as shown

by the $K_i$ values) on the damaged DNA template, whereas no nucleotide substrate inhibition was observed for pol $\beta$ (Table 1). Taken together, these results indicated that pol $\lambda$ has a higher affinity for the nucleotide substrate and a higher efficiency of AP site bypass than pol $\beta$.

*Pol $\beta$, but Not Pol $\lambda$, Can Bypass an AP Site by Two Alternative Mechanisms.* To investigate in more detail the mechanism of lesion bypass and −1 frameshift generation by pol $\lambda$ and pol $\beta$, single nucleotide incorporation experiments were performed with the 18/73mer DNA substrate (i.e., under standing start conditions). As shown in Figure 2A, when pol $\lambda$ was challenged with increasing dATP concentrations, no incorporation was detected, either in front of the G at position +1 of the undamaged template (lanes 2−7) or in front of the abasic site on the damaged template (lanes 14−19). On the other hand, when increasing concentrations of dCTP were added, the expected +2 nt product was efficiently synthesized on the undamaged template (lanes 8−13). Additional products of 3 and 4 nt in length also appeared. The 3 nt product could be generated through a nucleotide-stabilized primer misalignment, where, after incorporation of the first two C residues, the A at position +3 of the template is looped out, allowing incorporation of an additional C in front of the G at position +4. This event would generate a CCC primer terminal sequence. This sequence could then induce a primer slippage, where the first two C's are looped out and the primer anneals to the G at position +1 of the template, allowing the incorporation of an additional C in front of the G at position +2, thus explaining the appearance of the 4 nt product.

When the same experiment was performed with the damaged template (lanes 20−25), a strong accumulation of a +1 nt product along with products of +2 nt and +3 nt in length was detected. These results suggested that pol $\lambda$ bypassed the AP site through a nucleotide-stabilized primer misalignment mechanism, where the AP site is looped out and the G immediately downstream of the lesion is used as the templating base, resulting in a −1 frameshift, explaining why all of the products synthesized in the presence of the lesion were 1 nt shorter than the corresponding ones on the undamaged template.

The same experiment was performed with pol $\beta$. As shown in Figure 2B, and contrary to what was obtained with pol $\lambda$, pol $\beta$ showed detectable incorporation of dATP both in front of the G at position +1 of the undamaged template (lanes 1−6) or in front of the AP site on the damaged template (lanes 13−18). On the other hand, when dCTP was used as the nucleotide substrate, the expected +2 product was synthesized on the undamaged template (lanes 7−12), along with +3 nt and +4 nt products. This pattern was similar to the one observed with pol $\lambda$ (Figure 2A). Also similarly to pol $\lambda$, pol $\beta$ in the presence of dCTP (lanes 19−24) synthesized products on the damaged template which were 1 nt shorter than the ones on the undamaged template, that is, +1 nt, +2 nt, and +3 nt in length.

These results suggested that pol $\beta$ can bypass an AP site by two alternative mechanisms: first by a prominent one involving a nucleotide-stabilized primer misalignment mechanism, similar to the one displayed by pol $\lambda$, and second by a less efficient one, involving direct incorporation of A in front of the lesion.

Table 2: Kinetic Parameters for Single Nucleotide Incorporation on the 18/73mer DNA Substrate by DNA Polymerases $\lambda$ and $\beta$

| | Pol $\lambda$ | | | |
|---|---|---|---|---|
| | dCTP | | dATP | |
| | undamaged | AP damaged | undamaged | AP damaged |
| $K_m$ ($\mu$M) | 0.065 | 0.016 | nd | nd |
| $k_{cat}$ (min$^{-1}$) | 0.008 | 0.004 | nd | nd |
| $k_{cat}/K_m$ | 0.12 | 0.25 | nd | nd |
| $K_i$ ($\mu$M) | 880 | 107 | nd | nd |

| | Pol $\beta$ | | | |
|---|---|---|---|---|
| | dCTP | | dATP | |
| | undamaged | AP damaged | undamaged | AP damaged |
| $K_m$ ($\mu$M) | 0.14 | 2.3 | 250 | 167 |
| $k_{cat}$ (min$^{-1}$) | 0.025 | 0.008 | 0.004 | 0.04 |
| $k_{cat}/K_m$ | 0.17 | 0.003 | $1.6 \times 10^{-5}$ | $2.4 \times 10^{-4}$ |

| Relative Efficiency (Damaged vs Undamaged) | | |
|---|---|---|
| | dCTP | dATP |
| | $(k_{cat}/K_m)_{AP}/(k_{cat}/K_m)_C$[a] | $(k_{cat}/K_m)_{AP}/(k_{cat}/K_m)_C$ |
| pol $\lambda$ | 22.5 | nd |
| pol $\beta$ | 0.017 | 15 |

| Absolute Efficiency (Pol $\lambda$ vs Pol $\beta$) | | |
|---|---|---|
| | dCTP | dATP |
| | $(k_{cat}/K_m)\lambda/(k_{cat}/K_m)\beta$ | $(k_{cat}/K_m)\lambda/(k_{cat}/K_m)\beta$ |
| C | 0.7 | nd |
| AP | 83 | nd |

[a] AP = AP-damaged DNA; C = undamaged control DNA.

*Kinetic Analysis of Single Nucleotide Incorporation by Pol $\lambda$ and Pol $\beta$.* From the quantification of the products synthesized in the absence or in the presence of an AP site as a function of the nucleotide (dATP or dCTP) concentrations (Figure 2), the steady-state kinetic parameters of pol $\beta$ and pol $\lambda$ for single nucleotide incorporation during normal and translesion DNA synthesis could be calculated, and the values for the kinetic constants ($K_m$, $k_{cat}$, $k_{cat}/K_m$) are summarized in Table 2. Since pol $\lambda$ was again inhibited by high concentrations of dCTP (Figure 2A), the apparent inhibition constant ($K_i$) for this substrate inhibition effect was also derived by using the appropriate kinetic model (see Materials and Methods), and this value is also indicated in Table 2. From the comparison of the kinetic constants listed in Table 2, it could be concluded that pol $\beta$ and pol $\lambda$ displayed comparable apparent incorporation rate ($k_{cat}$) values for dCTP on the damaged template, but pol $\lambda$ in addition showed a 145-fold higher apparent affinity for dCTP with respect to pol $\beta$, as indicated by the $K_m$ values. As a result, when the relative efficiencies of dCTP incorporation ($k_{cat}/K_m$ values) were compared for the undamaged vs the damaged DNA template, pol $\lambda$ was 22.5-fold more efficient in replicating the damaged template, whereas pol $\beta$ displayed an opposite behavior, being almost 60-fold more efficient on the undamaged template. This translated into an 83-fold higher efficiency in dCTP incorporation past an AP site for pol $\lambda$ than for pol $\beta$. Pol $\beta$ efficiently discriminated between correct (C-G) versus incorrect (A-G) incorporation on the undamaged template ($f_{inc}/f_c = 9.5 \times 10^{-5}$, that is, about 10000-fold preference for the correct versus the incorrect base pair). However, on the damaged template the preference for dCTP incorporation over dATP was only 12.5-fold. These results indicated that pol $\lambda$ was more efficient than pol $\beta$ in bypassing an AP site, and this is likely due to an increase in

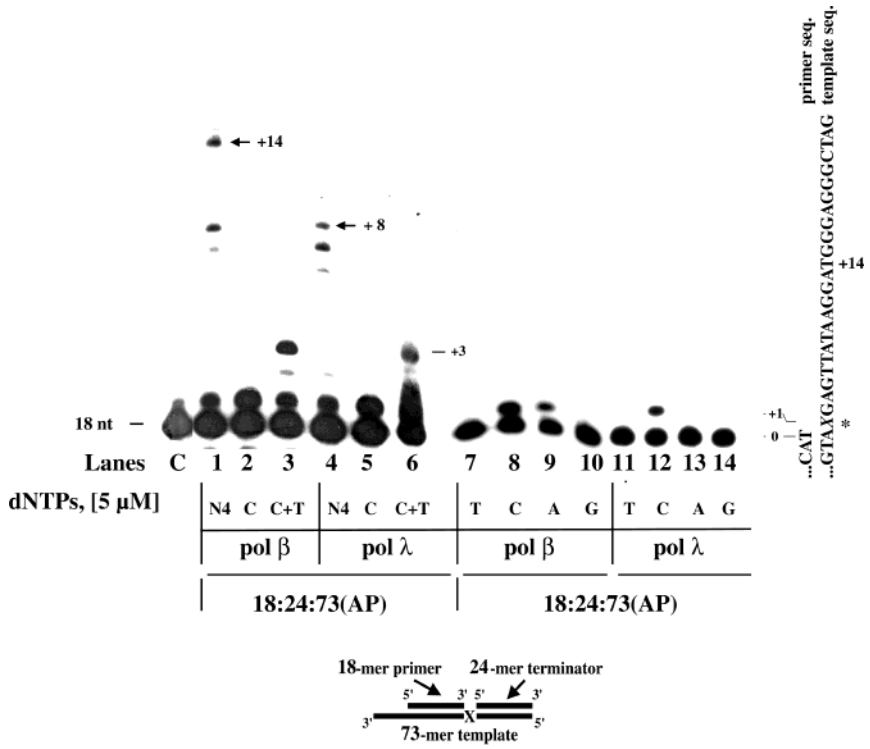


FIGURE 3: The mechanism of abasic site bypass by DNA polymerase $\beta$ and DNA polymerase $\lambda$ is not influenced by the structure of the DNA substrate. DNA primer elongation by 50 nM pol $\beta$ (lanes 1−3, 7−10) and 150 nM pol $\lambda$ (lanes 14−25) was measured under standing start conditions, as described in Materials and Methods, in the presence of 0.4 pmol of the 1 nt gapped 18/24/73mer heteropolymeric DNA primer/template containing an AP site and different combinations of dNTPs. Lane C shows the 18mer oligonucleotide size marker. Lanes: 1 and 4, 5 $\mu$M dNTPs;2, 5, 8, and 12, 5 $\mu$M dCTP; 3 and 6, 5 $\mu$M each dCTP and dTTP; 7 and 11, 5 $\mu$M dTTP; 9 and 13, 5 $\mu$M dATP; 10 and 14, 5 $\mu$M dGTP. Arrows indicate the length of the synthesized products. The asterisk indicates the position of the AP site. The sequence of the DNA template is indicated on the right side of the panel, and the schematic structure of the DNA substrate is represented on the bottom.

the apparent affinity for the incoming nucleotide in the presence of the AP site.

*The Mechanism of Abasic Site Bypass by Pol $\beta$ and Pol $\lambda$ Is Not Influenced by the Structure of the DNA Substrate.* It has been shown that both pol $\beta$ and pol $\lambda$ can efficiently utilize as substrate dsDNA containing short gaps (*9*, *23*). To test whether the presence of a double-stranded DNA tract downstream of the lesion was affecting the bypass mechanism of pol $\beta$ and pol $\lambda$, a 1 nt gapped template was constructed by annealing a 24-mer oligonucleotide complementary to the sequence downstream of the abasic site (positions +2 to +25). The schematic structure of this 18/24/73mer template is shown in the bottom of Figure 3. When all four dNTPs were present, both pol $\beta$ and pol $\lambda$ were able to synthesize products longer that the 1 nucleotide gap (indicated by arrows in lanes 1 and 4, respectively) even if shorter than the expected full-length product. This was likely due to a limited strand displacement activity earlier observed for both enzymes. Addition of dCTP only (lanes 2 and 5) resulted in the formation of a +1 product, likely due to looping out of the abasic site at position +1 and use of the G at position +2 as the templating base for the incoming nucleotide. If this was true, then performing the reaction in the presence of dCTP and dTTP should result in further elongation, due to the AG at positions +3 and +4 of the template sequence. As shown in lanes 3 and 6 of Figure 3, in the presence of both dCTP and dTTP, a 3 nt product appeared with both enzymes. According to the template sequence shown on the right side of the panel, this was the product expected from incorporation in front of the triplet -GAG- at positions +2 to +4 of the template.

Finally, the incorporation of each nucleotide alone by both enzymes was also tested. As can be seen, pol $\beta$ was able to incorporate both dCTP and dATP (lanes 8 and 9), whereas pol $\lambda$ showed dCTP incorporation only (lane 12). These results indicated that both pol $\beta$ and pol $\lambda$ were able to bypass an AP site on a 1 nt gapped DNA substrate by mechanisms similar to those observed with single- stranded DNA templates.

*The Template Slippage Mechanism of Pol $\lambda$ Is Influenced by the DNA Sequence Context.* The results shown in Figure 2A suggested that, under conditions leading to premature termination of DNA synthesis (i.e., in the presence of only one nucleotide), pol $\lambda$ could promote template slippage even in the absence of an abasic site. This could explain the additional products detected in Figure 2A, lanes 8−13, as well as the absolute preference for dCTP incorporation in the presence of the AP site, since the nucleotide in the template sequence immediately downstream of the lesion is a G. According to this interpretation, one would expect that the identity of the incoming nucleotide able to induce the template slippage changes as a function of the particular sequence context. To directly prove this, nucleotide incorporation by pol $\lambda$ was analyzed on a 20/60mer template having a different sequence than the 17/73 or 18/73 templates previously used (see Materials and Methods for the complete sequence of the primer/template). As shown in Figure 4A, for the undamaged template, not only correct dCTP incor-

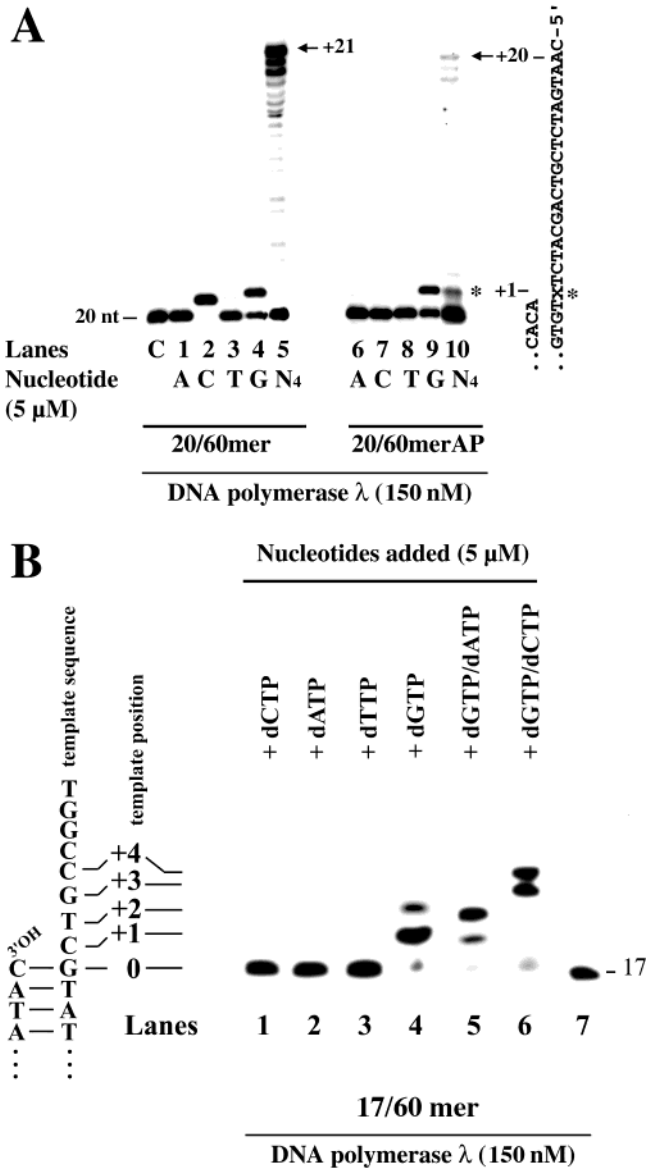


FIGURE 4: The template slippage mechanism of DNA polymerase λ is influenced by the DNA sequence context. (A) DNA primer elongation by pol λ was measured under standing start conditions, as described in Materials and Methods, in the presence of 0.2 pmol of the 20/60mer heteropolymeric DNA primer/template, either undamaged (lanes 1−5) or containing a single AP site (lanes 6−10), and in the presence of different combinations of dNTPs. Lane C shows the 20mer oligonucleotide size marker. Lanes: 1 and 6, 5 μM dATP; 2 and 7, 5 μM dCTP; 3 and 8, 5 μM dTTP; 4 and 9, 5 μM dGTP; 5 and 10, 5 μM dNTPs. Arrows indicate the length of the synthesized products. The concentration of the pol used is at the bottom of the figure. The asterisk indicates the position of the AP site. The sequence of the DNA template is indicated on the right side of the panel. X = G in the undamaged template or AP site in the damaged template. (B) DNA primer elongation by pol λ was measured under standing start conditions, as described in Materials and Methods, in the presence of 0.2 pmol of the 17/60mer heteropolymeric DNA primer/template and in the presence of different combinations of dNTPs. Lanes: 1, 5 μM dCTP; 2, 5 μM dATP; 3, 5 μM dTTP; 4, 5 μM dGTP; 5, 5 μM each dGTP and dATP; 6, 5 μM each dGTP and dCTP. Lane 7 shows the 17mer oligonucleotide size marker. The concentration of pol used is at the bottom of the figure. The sequence of the DNA template is indicated on the left side of the panel.

poration was observed in front of the G at position +1 (lane 2) but also incorporation of dGTP was detected, albeit with lower efficiency (lane 4). However, on the same template bearing an AP site at position +1, the preferred nucleotide incorporated by pol λ during translesion DNA synthesis was dGTP (lane 9), wheras no incorporation was observed with either dATP, dCTP, or dTTP (lanes 6−8). A full-length product of the expected size (+21 nt) was observed on the undamaged template in the presence of all four dNTPs (lane 5), whereas on the damaged template, a +20 nt product was synthesized, again suggesting that a −1 frameshift occurred (lane 10). According to the 20/60mer template sequence, these results indicated that template slippage occurred through preferential utilization of the C at position +3 for base pairing with an incoming dGTP (lanes 4 and 9), instead of usage of the T at position +2 for pairing with an incoming dATP (lanes 1 and 6). One possible explanation might be that the terminal primer nucleotides C and A reannealed to the template position +1 to +2 (GT), thus enabling the C at position +3 to base pair with the incoming dGTP.

To further characterize this homology-driven primer reannealing mechanism of template slippage by pol λ in the absence of the lesion, a 17mer primer was annealed to the 60mer undamaged substrate (see Materials and Methods for sequence details). As shown in Figure 4B, correct dGTP incorporation in front of the C at position +1 was observed along with an additional +2 product (lane 4). No incorporation was observed, on the other hand, in the presence of dATP, dCTP, or dTTP (lanes 1−3). When the first two encoded nucleotides (dGTP and dATP) were added to the reaction, only the expected +2 product was observed (lane 5). Interestingly, when dGTP and dCTP only were present, a 4 nt product could be readily synthesized by pol λ (lane 6). These results are in agreement with a template slippage mechanism which involved incorporation of the first G in front of the C at position +1 of the template, followed by a homology-driven primer reannealing of the resulting ACG primer terminus to positions +2 to +4 of the template strand, thus allowing the C at position +5 to serve as the template for incorporation of the second dGTP. Addition of dCTP together with dGTP allowed synthesis through the incorporation of two C residues in front of the GG sequence at positions +6 and +7 of the template strand, resulting in the 4 nt product (lane 6). On the other hand, in the presence of the correct nucleotides dGTP and dATP, the +2 product synthesized could not be further elongated (lane 5), since the resulting primer sequence ACGT lacked homology with the template sequence immediately downstream, preventing template slippage and primer reannealing. These results indicated that template slippage by pol λ proceeds through a homology-driven primer reannealing mechanism.

*Kinetic Analysis of the Template Slippage-Dependent DNA Synthesis by Pol λ.* As can be seen from Figure 4B, lane 4, a strong stop was present at position +1 when only G was added to the reaction. This suggested that the enzyme was pausing (and possibly dissociating) after the first G incorporation, before adding the second G residue. Such a strong pausing would be in agreement with the proposed template slippage mechanism, where incorporation of the first G must be followed by dissociation of the enzyme, primer reannealing, and incorporation of the second G. To more quantitatively investigate this model, time course experiments were performed on the 17/60mer primer/template in the presence of G only (Figure 5A). As can be seen, incorporation of the first G was very fast, with significant accumulation of +1

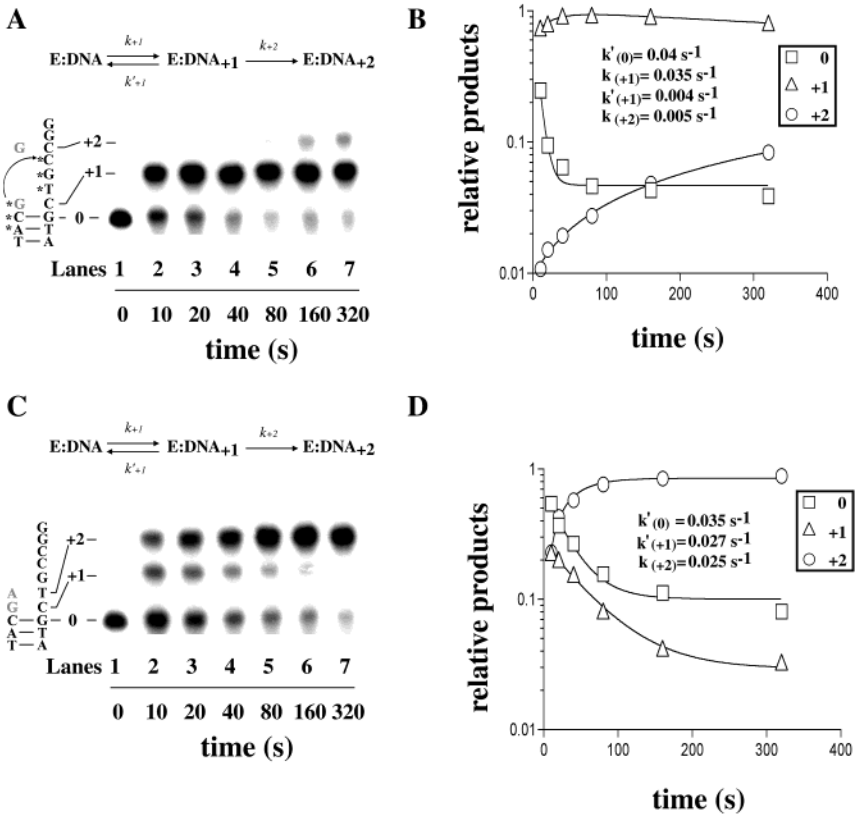


FIGURE 5: Kinetic analysis of the template slippage-dependent DNA synthesis by DNA polymerase $\lambda$. (A) Time-dependent DNA primer elongation by pol $\lambda$ (150 nM) was measured under standing start conditions, as described in Materials and Methods, in the presence of 0.2 pmol of the 17/60mer heteropolymeric DNA primer/template and in the presence of 5 $\mu$M dGTP. A minimal kinetic pathway is shown on top of the panel. The template sequence immediately downstream from the primer terminus is shown on the left side of the panel. Asterisks indicate the sequence homologous regions between primer and template (for explanation see text). (B) Quantification of the products shown in panel A. Data were fitted to the equation $A(e^{-k_{+1}t} - e^{k'_{+1}t})$ for the time-dependent accumulation and disappearance of the +1 (triangles) products, to the equation $A(1 - e^{-k_{+2}t})$ for the accumulation of the +2 (circles) products, and to the equation $A(e^{-k'_0t})$ for the disappearance of the 17mer primer (product 0, squares). In all cases $A$ is the amplitude factor and $t$ is time. (C) Time-dependent DNA primer elongation by pol $\lambda$ (150 nM) was measured under standing start conditions, as described in Materials and Methods, in the presence of 0.2 pmol of the 17/60mer heteropolymeric DNA primer/template and in the presence of 5 $\mu$M each dGTP and dATP. A minimal kinetic pathway is shown on top of the panel. The template sequence immediately downstream from the primer terminus is shown on the left side of the panel. (D) Quantification of the products shown in panel A. Data were fitted to the equation $A(1 - e^{-k_{+2}t})$ for the accumulation of the +2 (circles) products and to the equations $A(e^{-k'_{+1}t})$ for the disappearance of the +1 (triangles) products and $A(e^{-k'_0t})$ for the 17mer primer (product 0, squares).

product after 10 s (lane 2). Significant +2 nt product synthesis, corresponding to addition of a second G nucleotide, was detectable only at later time points (lanes 6 and 7). The products were quantified, and the relative band intensities were plotted as a function of the incubation time. As shown in Figure 5B, the kinetics of disappearance of the unreacted 18-mer primer (position 0) was the same as the kinetics of accumulation of the product +1. The apparent rate of primer decay ($k'_0$) was 0.04 ($\pm$0.01) $s^{-1}$, and the rate of accumulation of +1 ($k_{+1}$) was 0.035 ($\pm$0.005) $s^{-1}$. However, the +1 product showed a much slower decay rate ($k'_{+1}$) of 0.004 ($\pm$0.001) $s^{-1}$, which was comparable with the rate of accumulation of the product +2 ($k_{+2}$), which was 0.005 ($\pm$0.001) $s^{-1}$. These results suggested that the rate-limiting step was different for the second nucleotide addition with respect to the incorporation of the first nucleotide. The proposed model is shown on the left side of panel A, where the terminal -ACG sequence of the primer, resulting from the incorporation of the first G, can base pair with the -TGC- at positions +2 to +4 of the template, leading to incorporation of an extra G in front of position +5. This template slippage was likely induced by the lack of the correct next encoded nucleotide, which, according to the template sequence, was an A. To directly test this, time course experiments of nucleotide incorporation by pol $\lambda$ were performed on the 17/60mer primer/template in the presence of both G and A nucleotides. As shown in Figure 5C, significant accumulation of +2 product was already detectable after 10 s, and complete conversion of product +1 into product +2 was achieved after 160 s. No extra nucleotide addition was observed. This was in agreement with the mechanism proposed on the left side of panel C. After subsequent incorporation of the correct nucleotides G and A, the resulting -CGA primer terminus did not have significant homology with the downstream template sequence, thus preventing the possibility of template slippage and primer reannealing. The products were quantified, and the relative band intensities were plotted as a function of the incubation time. As shown in Figure 5D, the accumulation rate of the product +1 ($k_{+1}$) was too fast to be measured; thus only the apparent rates of decay of the 18mer primer ($k'_0$) and of the +1 product ($k'_{+1}$) could be estimated, together with the apparent accumulation rate of the product +2 ($k_{+2}$). However, all of the rate values were comparable, indicating that there was only one rate-limiting step for both the first and the second nucleotide incorporation events. In summary,

these kinetic data suggested that the extra nucleotide addition by pol $\lambda$ occurred with different (and slower) kinetics than correct nucleotide incorporation, thus in agreement with a template slippage-mediated mechanism.

## DISCUSSION

It has been shown that AP site bypass by pol $\beta$ occurred predominantly by a dNTP-stabilized mechanism, analogous to but different from the classical template slippage, resulting in both deletion and base substitution errors (*15*). In this work we present in vitro data indicating that pol $\lambda$, when compared to pol $\beta$ on the same substrates and under the sameexperimental conditions, also preferentially uses this mechanism for AP site bypass, generating a $-1$ frameshift (Figure 1). However, several important differences could be observed. First, pol $\beta$ bypassed the AP site also by incorporating an A in front of the lesion, with about 10-fold lower efficiency with respect to the "lesion-skipping" mechanism, while such a mode of translesion synthesis could not be observed for pol $\lambda$ (Figure 2). Second, both under running and standing start conditions, pol $\lambda$ could incorporate nucleotides on the damaged DNA with the same or even a higher efficiency than on the undamaged DNA, whereas pol $\beta$ activity was greatly reduced in the presence of the lesion (Tables 1 and 2). As a result, pol $\lambda$ had a higher efficiency in bypassing an AP site than pol $\beta$. Third, the apparent affinity for the nucleotide substrate was increased for pol $\lambda$ by the presence of an AP site on the template strand, whereas the opposite was observed for pol $\beta$. Moreover, pol $\lambda$ was inhibited by dNTPs concentrations above 60 $\mu$M during translesion synthesis, whereas pol $\beta$ required high dNTP concentrations for efficient lesion bypass (Tables 1 and 2).

Another interesting observation was that pol $\lambda$ was able to promote template slippage in the absence of a lesion but under conditions of forced termination of DNA synthesis, for example, when only one nucleotide was present in the reaction (Figures 4 and 5). This occurred through two different mechanisms: (i) by a dNTP-stabilized mechanism, similar to the one already described for pol $\beta$, where the presence of an incoming dNTP complementary to the template base downstream from the forced termination site is sufficient to cause misalignment incorporation to take place and (ii) by an homology-driven primer reannealing mechanism, where reannealing of the terminal sequence of primer to a homologous region further downstream along the template allows incorporation to take place.

These results led us to propose a model (Figure 6) where we suggest that, among the different possible misaligned DNA structures, the most thermodynamically stable is always favored by pol $\lambda$. Figure 6A shows the case of abasic site bypass with the template 20/60mer. With this template pol $\lambda$ preferentially used the homology between the last nucleotide of the primer (A) and the one downstream the lesion (T, position $+2$) to insert a G in front of the C at position $+3$ using an homology-driven primer reannealing mechanism, instead of inserting directly an A in front of the T at position $+1$ through a dNTP-stabilized primer misalignment (see Figure 4A for comparison). As indicated in the picture represented in the bubble of Figure 6A, this can be explained by the fact that, in the case of dGTP incorporation, the extrahelical residues are stabilized by five hydrogen bonds,

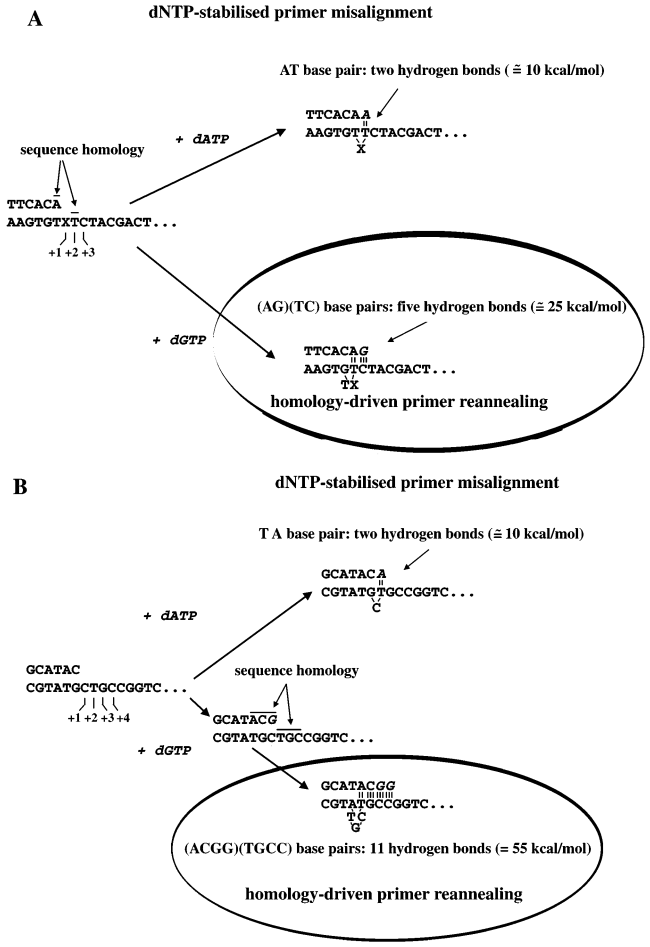


FIGURE 6: Thermodynamic stability dictates the choice between alternative mechanisms of template slippage. (A) Bypass of the lesion (shown as an X in the template sequence) can occur either through a dNTP-stabilized mechanism (upper right part of the panel) or through a homology-driven primer reannealing mechanism (bubbled, lower right). The number of hydrogen bonds available to stabilize the resulting extrahelical bases determines which mechanism is preferred (in this example the lower one). (B) Template slippage in the absence of a lesion can occur either through a dNTP-stabilized mechanism (upper right part of the panel) or through a homology-driven primer reannealing mechanism (bubbled, lower right). The number of hydrogen bonds available to stabilize the resulting extrahelical bases determines which mechanism is preferred (in this example the lower one). For further details see Discussion.

instead of the two for dATP incorporation (see alternative picture).

The same could also be observed in the absence on a lesion, for example, with the DNA substrate 17/60mer (Figure 6B). After incorporation of the first encoded nucleotide (dGTP), pol $\lambda$ was able to add an extra dGTP by using the sequence homology between the newly synthesized primer terminus (ACG) and the template positions $+2$ to $+4$. In this case, the extrahelical sequence is stabilized by a great number of hydrogen bonds (see representation in bubble of Figure 6B). However, in the presence of dATP only, pol $\lambda$ was not able to promote a dNTP-stabilized primer misalignment due to the limited stability of the resulting extrahelical structure (see alternative picture in Figure 6B and also Figure 4B).

In summary, our data suggested that, in the presence of microhomology between the primer and the template strand

downstream of the first position, pol λ can spontaneously promote template slippage, generating −1 frameshift mutations, thus providing a molecular explanation for the observed mutation spectrum of pol λ in vivo (*10*). These remarkable features of pol λ are likely the consequences of its particular mode of DNA binding. When the structure of pol λ complexed with a two nucleotide gapped DNA was compared to the structures of pol β in complex with a one nucleotide gapped DNA substrates, it could be seen that the upstream DNA strand was shifted one nucleotide away from the pol λ active site (*11*). Thus, the templating base occupied a position corresponding to that of the +1 template base in the pol β structure so that the pol λ residues equivalent to those in pol β that interact with the templating residue interacted instead with the next template residue, i.e., the one adjacent to the downstream duplex in the two nucleotide gap (*11*). This particular conformation could also explain the intrinsic ability of pol λ to promote homology searching and pairing between two DNA strands, supporting its suggested functional role in the nonhomologous end joining process (*24*).

A yet unanswered question is whether pol λ participates in DNA repair and or replication processes as part of a multiprotein complex. Even though several lines of evidence point to the existence of such specialized multiprotein complexes, pol λ has not been reported yet as a component of any of these. However, an indication that pol λ might be present in the cell in association with other proteins comes from the recent data showing that it can interact both physically and functionally with PCNA (*16*), a protein which is involved in many DNA repair and replication processes. The fact that PCNA promotes the translesion activity of pol λ past an abasic site might suggest that this specialized function of pol λ will be mantained also within a larger multiprotein complex, even though we cannot exclude that additional factors may influence the biochemical properties of pol λ in vivo.

## ACKNOWLEDGMENT

We thank Dr. L. Blanco for kindly providing us with the expression plasmid for recombinant human pol λ.

## REFERENCES

1. Hubscher, U., Maga, G., and Spadari, S. (2002) Eukaryotic DNA polymerases, *Annu. Rev. Biochem. 71*, 133−163.
2. Davies, J. F., Almassy, R. J., Hostomska, Z., Ferre, R. A., and Hostomsky, Z. (1994) 2.3 Å crystal structure ot the catalytic domain of DNA polymerase β, *Cell 76*, 1123−1133.
3. Sawaya, M. R., Pelletier, H., Kumar, A., Wilson, S. H., and Kraut, J. (1994) Crystal structure of rat DNA polymerase beta: evidence for a common polymerase mechanism *Science 264*, 1930−1935.
4. Pelletier, H., Sawaya, M. R., Wolfle, W., Wilson, S. H., and Kraut, J. (1996) Crystal structures of human DNA polymerase beta complexed with DNA: implications for catalytic mechanism, processivity, and fidelity, *Biochemistry 35*, 12742−12761.
5. Sawaya, M. R., Prasad, R., Wilson, S. H., Kraut, J., and Pelletier, H. (1997) Crystal structures of human DNA polymerase beta complexed with gapped and nicked DNA: evidence for an induced fit mechanism, *Biochemistry 36*, 11205−11215.
6. Blanca, G., Shevelev, I., Ramadan, K., Villani, G., Spadari, S., Hubscher, U., and Maga, G. (2003) Human DNA polymerase lambda diverged in evolution from DNA polymerase beta toward specific Mn(++) dependence: a kinetic and thermodynamic study, *Biochemistry 42*, 7467−7476.
7. Shevelev, I., Blanca, G., Villani, G., Ramadan, K., Spadari, S., Hubscher, U., and Maga, G. (2003) Mutagenesis of human DNA polymerase lambda: essential roles of Tyr505 and Phe506 for both DNA polymerase and terminal transferase activities, *Nucleic Acids Res. 31*, 6916−6925.
8. Ramadan, K., Maga, G., Shevelev, I. V., Villani, G., Blanco, L., and Hubscher, U. (2003) Human DNA polymerase lambda possesses terminal deoxyribonucleotidyl transferase activity and can elongate RNA primers: Implications for novel functions, *J. Mol. Biol. 328*, 63−72.
9. Garcia-Diaz, M., Bebenek, K., Sabariegos, R., Dominguez, O., Rodriguez, J., Kirchhoff, T., Garcia-Palomero, E., Picher, A. J., Juarez, R., Ruiz, J. F., Kunkel, T. A., and Blanco, L. (2002) DNA polymerase lambda, a novel DNA repair enzyme in human cells, *J. Biol. Chem. 277*, 13184−13191.
10. Bebenek, K., Garcia-Diaz, M., Blanco, L., and Kunkel, T. A. (2003) The frameshift infidelity of human DNA polymerase lambda. Implications for function, *J. Biol. Chem. 278*, 34685−34690.
11. Garcia-Diaz, M., Bebenek, K., Krahn, J. M., Blanco, L., Kunkel, T. A., and Pedersen, L. C. (2004) A structural solution for the DNA polymerase lambda-dependent repair of DNA gaps with minimal homology, *Mol. Cell 13*, 561−572.
12. Delarue, M., Boule, J. B., Lescar, J., Expert-Bezancon, N., Jourdan, N., Sukumar, N., Rougeon, F., and Papanicolaou, C. (2002) Crystal structures of a template-independent DNA polymerase: murine terminal deoxynucleotidyltransferase, *EMBO J. 21*, 427−439.
13. Beard, W. A., and Wilson, S. H. (2001) DNA lesion bypass polymerases open up, *Structure (Cambridge) 9*, 759−764.
14. Yang, W. (2003) Damage repair DNA polymerases Y, *Curr. Opin. Struct. Biol. 13*, 23−30.
15. Efrati, E., Tocco, G., Eritja, R., Wilson, S. H., and Goodman, M. F. (1997) Abasic translesion synthesis by DNA polymerase beta violates the "A-rule". Novel types of nucleotide incorporation by human DNA polymerase beta at an abasic lesion in different sequence contexts, *J. Biol. Chem. 272*, 2559−2569.
16. Maga, G., Villani, G., Ramadan, K., Shevelev, I., Le Gac, N. T., Blanco, L., Blanca, G., Spadari, S., and Hubscher, U. (2002) Human DNA polymerase lambda functionally and physically interacts with proliferating cell nuclear antigen in normal and translesion DNA synthesis, *J. Biol. Chem. 277*, 48434−48440.
17. Lindahl, T., and Wood, R. D. (1999) Quality control by DNA repair, *Science 286*, 1899−1905.
18. Lindahl, T., Karran, P., and Wood, R. D. (1997) DNA excision repair pathways, *Curr. Opin. Genet. Dev. 7*, 158−169.
19. Dianov, G. L., Sleeth, K. M., Dianova, II, and Allinson, S. L. (2003) Repair of abasic sites in DNA, *Mutat. Res. 531*, 157−163.
20. Taylor, J. S. (2002) New structural and mechanistic insight into the A-rule and the instructional and noninstructional behavior of DNA photoproducts and other lesions, *Mutat. Res. 510*, 55−70.
21. Ling, H., Boudsocq, F., Woodgate, R., and Yang, W. (2004) Snapshots of replication through an abasic lesion; structural basis for base substitutions and frameshifts, *Mol. Cell 13*, 751−762.
22. Hogg, M., Wallace, S. S., and Doublie, S. (2004) Crystallographic snapshots of a replicative DNA polymerase encountering an abasic site, *EMBO J. 23*, 1483−1493.
23. Beard, W. A., and Wilson, S. H. (2000) Structural design of a eukaryotic DNA repair polymerase: DNA polymerase beta, *Mutat. Res. 460*, 231−244.
24. Lee, J. W., Blanco, L., Zhou, T., Garcia-Diaz, M., Bebenek, K., Kunkel, T. A., Wang, Z., and Povirk, L. F. (2004) Implication of DNA polymerase lambda in alignment-based gap filling for nonhomologous DNA end joining in human nuclear extracts, *J. Biol. Chem. 279*, 805−811.

BI049050X